*Journal of the European Ceramic Society* **16** (1996) 1035–1039

PII: S0955-2219(96)00029-5
0955-2219/96/$15.00

# β-Conductivity Contrast at Barium Titanate Thermistor Grain Boundaries

J. D. Russell & C. Leach

Manchester Materials Science Centre, University of Manchester and UMIST, Grosvenor Street, Manchester, M1 7HS, UK

(Received 15 August 1995; revised version received 11 January 1996; accepted 12 January 1996)

***Abstract***

*Barium titanate based PTC thermistor materials have been examined using the conductive mode of a scanning electron microscope. Under an applied voltage bias, at temperatures above the Curie temperature, bright and dark lines which are due to β-conductivity appear coincident with grain boundaries. The mechanisms of contrast formation are discussed. Such contrast can be used to evaluate the distribution of this type of active grain boundary.*
*© 1996 Elsevier Science Limited.*

## 1 Introduction

The positive temperature coefficient (PTC) of resistance properties of barium titanate ceramics and similar materials has long been used for applications such as thermal protection and current-limiting devices.[1,2] Early models of the PTC effect invoked double Schottky barriers at grain boundaries due to a build-up of negatively charged acceptor states at the interface.[3] This gives rise to a potential barrier whose height at a given temperature depends on the dielectric constant, which changes rapidly around the Curie temperature ($T_c$). Extensions to this model by Jonker included the spontaneous polarization which occurs below $T_c$ and reduces the expected potential barrier height.[4] Daniels and Wernicke[5] modelled the behaviour by considering an extended grain boundary layer in which the donor dopants are heavily compensated by barium vacancies, frozen-in during cooling from the sintering temperature. In practice, these models are still the subject of some debate,[6] and probably only represent special cases of the overall situation, with microstructural heterogeneity also being an issue in considering the overall electrical properties of electronic ceramics.[7]

Remote electron beam induced current (REBIC) is a specialized form of conductive mode microscopy, which essentially involves making two connections to the sample: one to earth, and one through a current amplifier to earth. The images and line-scans formed with the amplified output may show contrast due to three main mechanisms:

(I) *charge collection* due to separation of generated electron-hole pairs at built-in fields and their subsequent collection at the electrodes,[8]
(II) *β-conductivity*, a direct analogue of photoconductivity, due to the localized injection of charge carriers by the electron beam and increased local conductivity observed under voltage bias,[9,10] and
(III) *resistive contrast* due to the specimen acting as a current divider for the absorbed beam current to travel to earth[11] and non-linear resistance variations, giving a signal step at resistive barriers.

Resistive contrast is observed to some extent at most grain boundaries, and is rather weak, as the signal containing this effect is necessarily smaller than the beam current. The other two contrast types are caused by the electron-hole pairs generated by the electron beam, and as the electron beam energy is orders of magnitude greater than the electron-hole pair formation energy, each beam electron generates thousands of electron-hole pairs in the sample. The resulting signals are therefore much stronger than those due to resistive contrast. According to Heywang's model,[3] the grain boundary is characterized by interface charge which gives rise to a back-to-back Schottky diode structure. It is the electric field due to band bending associated with these barrier structures which can give rise to electron-hole pair separation and subsequent collection, resulting in contrast due to the first mechanism described above. The n–i–n grain boundary structure of Daniels' model has two regions of band-bending, which are separated by a boundary layer.

The REBIC technique has recently been applied to the study of electronic ceramic materials such as zinc oxide[12,13] and barium titanate.[14] REBIC offers one of the few means of visualizing such electrical properties

at individual grain boundaries. In this contribution, we describe $\beta$-conductivity contrast in PTC thermistors, an effect that has not previously been reported in these materials.

## 2 Method

Commercial barium titanate PTC thermistor material was cut into 1 mm thick sections and polished on nylon cloth using a water-based slurry of 0·3 $\mu$m $\alpha$-alumina powder. Electrical contacts were formed by evaporating aluminium through a fine transmission electron microscope grid to form an array of closely spaced contacts. After mounting the samples on insulating stubs they were observed in a scanning electron microscope (SEM) fitted with an Oxford Instruments H1001 heating stage. Micromanipulator probes, attached through the side port of the SEM, were then placed directly in contact with the electrodes, and the collected REBIC signal amplified with a high-sensitivity current amplifier for both imaging and quantitative linescans.

## 3 Results

At room temperature the specimen resistance is very small and REBIC images are very noisy due to instrumentation considerations.[14] However, on

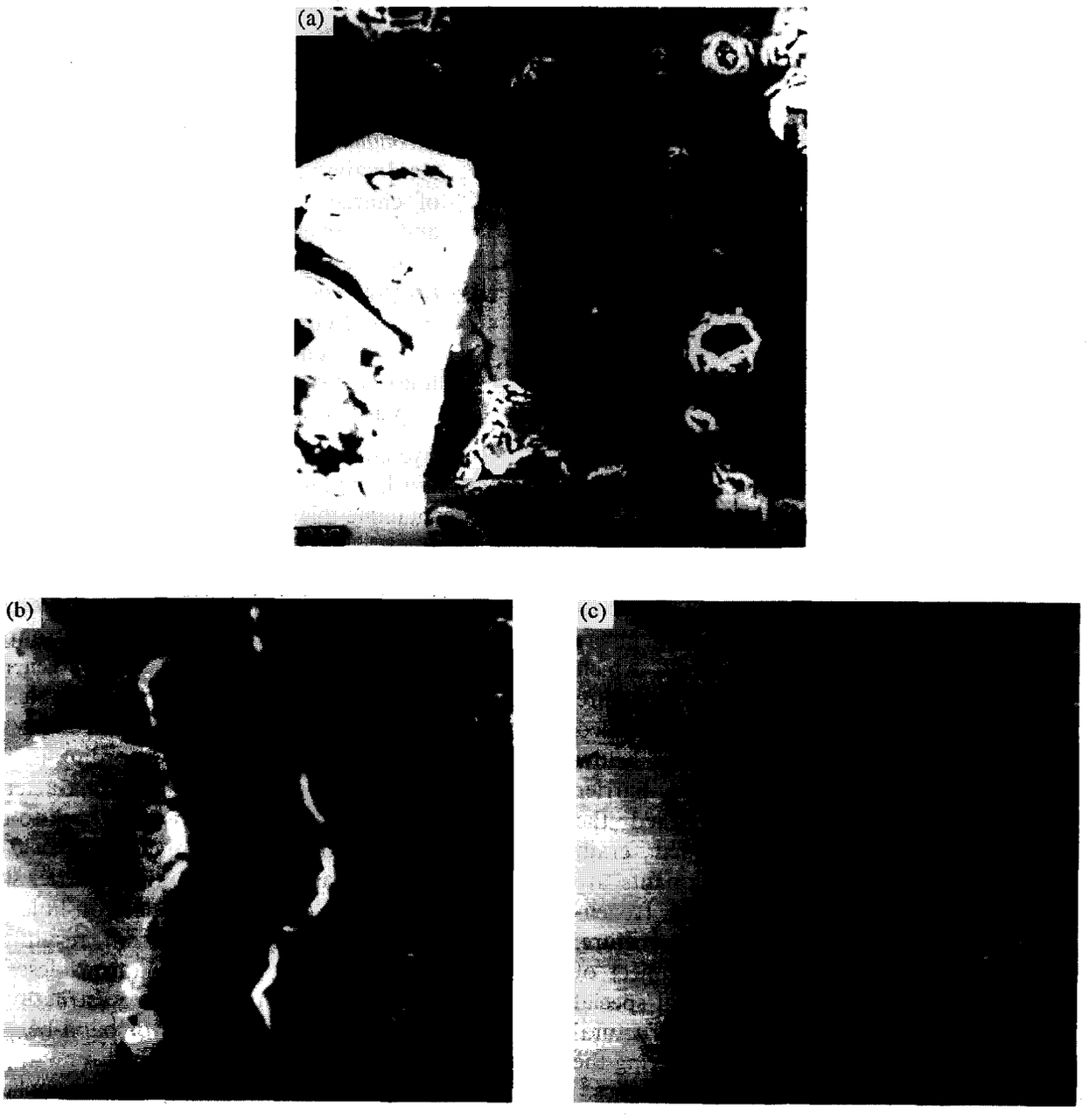


**Fig. 1.** SE (a) and REBIC images (b,c) taken at 180°C with biases of +0·161 V and –0·054 V respectively, showing a reversal in the $\beta$-conductivity contrast. The two aluminium contact pads can be seen on the left and right of the images, while one of the probes can be seen on the visible area of the left contact. The scale bar indicates 20 $\mu$m.

heating samples *in situ* above the Curie transition temperature, the specimen resistance becomes large enough to facilitate high-quality imaging of the electrical activity at the grain boundaries.

Previous studies have shown principally resistive contrast in this system, giving rise to a step in the signal level as the grain boundary is traversed by the electron beam scanning between the contacts,[14] and this effect is also observed in the samples described here. However, under an applied bias bright or dark lines also appear, coincident with some, but not all, grain boundaries [Figs 1(a) and (c)]. These lines are not due to any feature in the secondary or backscattered image of the SEM [Fig. 1(b)]. Often, the grain boundaries which show this contrast are those which are aligned transversely in the gap between the electrodes [on the left and right in Figs 1(b) and (c)], an orientation which corresponds geometrically to the maximum electric field gradient. It is also apparent that reversing the bias reverses the contrast at all active grain boundaries. For a given bias, only dark *or* bright contrast is observed. Notwithstanding the difficulties of imaging low-resistance samples, on decreasing the temperature towards the Curie temperature it is found that the contrast is steadily reduced until at the Curie temperature it has disappeared.

Quantitative linescans taken across an active grain boundary with positive and negative biases are shown in Fig. 2. The axes are offset to compensate for the large standing currents which flow between the contacts through the sample due to the applied bias. In these cases, the excess current which flows when the beam is incident at the grain boundary, $I_{gb}$, is about 15 nA, compared with the beam current of 1·6 nA.

## 4 Discussion

Polycrystalline materials often show bright or dark contrast caused by built-in fields at the

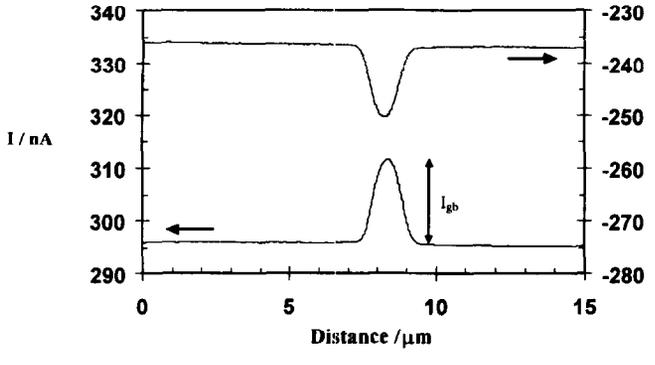


**Fig. 2.** REBIC linescans across a grain boundary like those shown in Fig. 1, with applied biases of +0·2 V and −0·2 V, and a beam current of 1·6 nA. The vertical scales of the two curves are offset to allow for the relatively large standing currents which flow.

Schottky barriers, due to charged grain boundary interface states. This contrast has been well characterized in silicon,[15] and several other semiconductors,[16,17] and has also been observed recently in electronic ceramics such as zinc oxide.[12] Such contrast consists of characteristic parallel bright and dark lines at a single grain boundary, although recently single line contrast which might also be due to built-in fields has been observed in such systems[13]

It would appear that the contrast observed here is due to β-conductivity rather than charge collection (of electron-hole pairs separated by built-in fields) for a number of reasons. Firstly, with no applied bias, it is very weak, and the contrast which does occur can be nulled completely to give a flat linescan profile by applying a very small bias (~mV) to compensate for the amplifier input offset voltage. Secondly, the contrast reversal with change in sign of the applied bias (which occurs for Schottky barrier contrast) would be accompanied by a lateral shift equal to the width of the electron beam excitation volume,[12] but no such shift is observed in these PTC thermistors. It is therefore concluded that the observed contrast is due to some form of enhanced conductivity induced by the electron beam. Since no type I contrast was observed here even though band bending is expected at both back-to-back Schottky barrier and n–i–n structures, we must conclude that either the band bending is too small to permit adequate charge separation or, more likely, that the generated electron-hole pairs recombine in and near the depletion region before becoming completely separated. This would make the charge collection currents too weak to be observed.

β-Conductivity depends on variations in the local resistivity under irradiation by the electron beam, and is a direct analogue of photoconductivity.[18] In the semiconducting grains of barium titanate, the conductivity $\sigma$ is given by:

$$\sigma = e(n\mu_e + p\mu_h) \quad (1)$$

where $e$ is the electronic charge, $n$ and $p$ are the carrier concentrations and $\mu_e$ and $\mu_h$ are the mobilities of electrons and holes, respectively. The generation of electron-hole pairs by the impinging electron beam increases the local carrier concentration, leading to a localized conductivity increase. When the beam is incident within the grains this effect is relatively small, because the carrier concentration is already large due to oxygen vacancies and aliovalent impurities which give strong $n$-type doping. At the grain boundaries, however, the conductivity is much smaller due to the barriers caused by charged grain boundary acceptor states,

and perhaps also by the presence of an intrinsic layer. In addition, lattice disorder, the presence of impurities and possibly also thin intergranular phases will reduce the carrier mobility. The local injection of excess electron-hole pairs can increase this grain boundary conductivity drastically either by simply increasing the number of carriers available for transport [eqn (1)] or by lowering the barrier itself when holes drift in the grain boundary electric fields to cause a transient, local neutralization of the grain boundary acceptor states.[19] Hence, although well above the Curie temperature grain boundary resistance is very large, it can be drastically reduced by electron-beam generated carriers, and give rise to a local increase in the current which flows under applied bias.

To describe how $I_{gb}$ depends on the beam current and the applied bias, we assumed a simple, linear model of grains with low resistivity and grain boundaries with very high resistivity. Assuming that the excess carrier concentration (hence conductivity increment) at the grain boundary is proportional to the beam current $I_b$, it can be shown (Appendix A) that the expected variation of $I_{gb}$ with beam current for the $\beta$-conductivity effect is of the form:

$$I_{gb} \propto \frac{V}{K + \frac{1}{I_b}} \qquad (2)$$

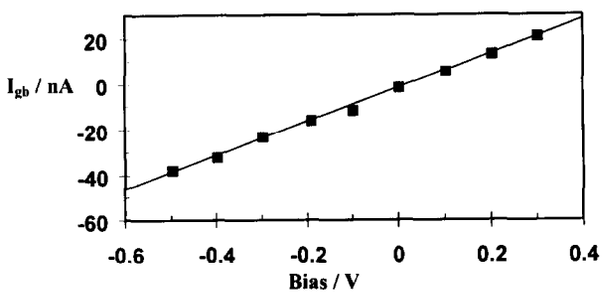


**Fig. 3.** Variation of the excess current which flows when the electron beam is incident at an active grain boundary, $I_{gb}$ (see Fig. 2), as a function of applied bias.

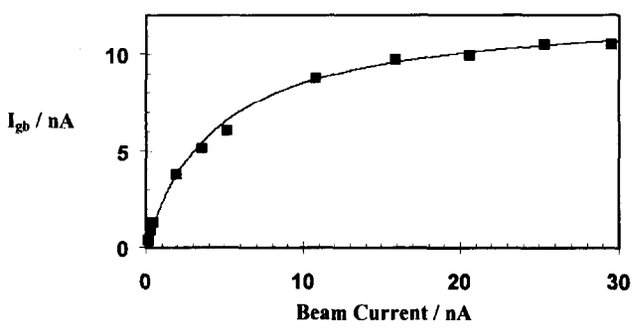


**Fig. 4.** Variation of $I_{gb}$ with the beam current. The solid line is fitted to the expected form given by eqn (2).

where $K$ is a constant and $V$ is the applied bias. The experimental variation of $I_{gb}$ with bias at constant beam current is shown in Fig. 3 and is linear, and hence consistent with eqn (2). The variation of $I_{gb}$ with the beam current at constant bias was also measured (Fig. 4), and a best-fit line calculated using eqn (2). It can be seen that the predicted relationship is followed closely by the experimental measurements. At high beam currents $I_{gb}$ saturates, since in this regime the resistivity of the thin insulating layer is sufficiently decreased by the electron beam that the overall sample resistance is dominated by grain resistances alone.

## 5 Conclusions

We have reported $\beta$-conductivity contrast in barium titanate PTC thermistor material for the first time, and discussed mechanisms by which it might arise. It provides a means of observing directly individual grain boundaries which are electrically active in this way.

The REBIC technique provides a very sensitive means by which many electrical properties of individual electronic ceramic grain boundaries can be characterized and compared, and is expected to become an important technique for studies of material behaviour and heterogeneity in the future.

## References

1. Saburi, O. & Wakino, K., Processing techniques and applications of positive temperature coefficient thermistors. *IEEE Trans. Compon. Parts*, **CP-10** (1963) 53–67.
2. Kulwicki, B. M., Trends in PTC resistor technology. *SAMPE J.*, **23**[6] (1987) 34–38.
3. Heywang, W., Resistivity anomaly in doped barium titanate. *J. Am. Ceram. Soc.*, **47** (1964) 484–490.
4. Jonker, G. H., Some aspects of semiconducting barium titanate. *Sol. St. Electron.*, **7** (1964) 895–903.
5. Daniels, J. & Wernicke, R., New aspects of an improved PTC model. *Philips Res. Repts*, **31** (1976) 544–559.
6. Chiang, Y.-M. & Takagi, T., Grain-boundary chemistry of barium titanate and strontium titanate II, Origin of electrical barriers in positive-temperature coefficient thermistors. *J. Am. Ceram. Soc.*, **73**[11] (1990) 3286–3291.
7. Abelard, P., Present understanding of the grain boundary electrical characteristics of semiconducting $BaTiO_3$ and $SrTiO_3$ ceramics. In *Electroceramics IV*, eds R. Waser, S. Hoffmann, D. Bonnenberg & Ch. Hoffmann. Augustinus Buchhandlung, Aachen, Germany, 1994, pp. 541–548.
8. Holt, D. B., The conductive mode. In Microcharacterisation of Semiconductors, eds D. B. Holt & D. C. Joy. Academic Press, London, 1989, Ch. 6.
9. Munakata, C., An application of beta conductivity to measurement of resistivity distribution. *J. Sci. Instr. (J. Phys. E) Series 2*: **1** (1968) 639–642.
10. Gopinath, A., On scanning electron microscope conduction-mode signals in bulk semiconductor devices: linear geometry. *J. Phys. D. Appl. Phys.*, **3** (1970) 467–472.

11. Smith, C. A., Bagnell, C. R., Cole, E. I., Dibianca, F. A., Johnson, D. G., Oxford, W. V. & Propst, R. H., Resistive contrast imaging: a new SEM mode for failure analysis. *IEEE Trans. El. Dev.*, **ED-33** (1986) 282–284.
12. Russell J. D., Halls, D. C. & Leach, C., Direct observation of grain boundary Schottky barrier behaviour in zinc oxide varistor material. *J. Mater. Sci. Lett.*, **14** (1995) 676–678.
13. Russell, J. D. & Leach, C., Direct observation of grain boundary electrical activity in PTCR thermistor material using the REBIC mode of the SEM. In *Proc. IVth Eur. Ceram. Soc. Conf., Vol. 5 — Electroceramics*, pp. 45–66.
14. Russell, J. D. & Leach, C., Problems associated with imaging resistive barriers in $BaTiO_3$ PTC ceramics using the SEM conductive mode. *J. Eur. Ceram. Soc.*, **15** (1995) 617–622.
15. Palm, J., Local investigation of recombination at grain boundaries in silicon by grain boundary-electron beam induced current. *J. Appl. Phys.*, **74** (1993) 1169–1178.
16. Mataré, H. F. & Laakso, C. W., Space-charge domains at dislocation sites. *J. Appl. Phys.*, **40** (1969) 476–482.
17. Bubulak, L O. & Tennent, W. E., Observation of charge separating defects in HgCdTe using remote contact electron beam induced current. *Appl. Phys. Lett.*, **52** (1988) 1255–1257.
18. Sze, S. M., *Physics of Semiconductor Devices*, 2nd edn. J. Wiley, New York, 1981, p. 744.
19. Palm, J., Steinbach, D. & Alexander, H., Local investigation of the electrical properties of grain boundaries. *Mater. Sci. Eng.*, **B24** (1994) 56–60.


## Appendix A: Derivation of Eqn (2)

We assume that the current path between the contacts can be treated one-dimensionally, and that there are two types of material:

(i) grain interiors consisting of extrinsic semiconductor with a high electron concentration; and
(ii) grain boundaries which have very low electron concentration.

The configuration we shall consider is shown in Fig. A1, from which we can write the total resistance between the contacts for the current path which traverses the grain boundary as:

$R = R_g + R_{gb}$ without the beam
$R' = R_g + R'_{gb}$ with the beam incident at the grain boundary

where $R_g$ is the resistance which is unchanged by the beam and $R_{gb}$ is the resistance at the grain boundary of interest. Throughout, priming indicates the new value of a variable when the electron beam is incident at the grain boundary. The excess current which flows due to the beam is given by:

$$I_{gb} = I' - I = \frac{V}{R_g + R'_{gb}} - \frac{V}{R_g + R_{gb}}$$

$$= V\left(\frac{R_{gb} - R'_{gb}}{(R_g + R_{gb})\,(R_g + R'_{gb})}\right) \qquad (A.1)$$

where $I$ and $V$ are the current through and potential difference across the structure under consideration (Fig. A1). In a real material, additional current will flow by other parallel current paths, but as such currents do not change when the beam is incident at the grain of interest, $I_{gb}$ is unaffected.

Under low injection conditions, the effect of the electron beam is to increase the equilibrium free electron concentration $n_0$ by an amount $\hat{n}$ which is proportional to $I_b$:

$$\hat{n} = \left(\frac{k}{e\mu}\right) I_b \quad (k \text{ is a constant})$$

Thus, eqn (1) becomes

$$\sigma' = (n_0 + \hat{n})e\mu = n_0 e\mu = kI_b$$

and

$$R'_{gb} = \frac{d}{A(n_o e\mu + kI_b)} = \frac{R_{gb}}{1 + kI_b} \qquad (A.2)$$

where $d$ is the thickness of the grain boundary layer, and $A$ is the area of the grain boundary which is affected by the beam. In addition, it should be noted that when the beam is incident in a grain $n_0$ is already high, so that the change in carrier concentration has a negligible effect on $\sigma$, hence such regions show no change of $I_{gb}$.
Substituting eqn (A.2) into eqn (A.1) gives:

$$I_{gb} = V\left(\frac{R_{gb} - \dfrac{R_{gb}}{1 + kI_b}}{(R_g + R_{gb})\left(R_{gb} + \dfrac{R_{gb}}{1 - kI_b}\right)}\right)$$

$$= V\left(\frac{R_{gb} kI_b}{(R_g + R_{gb})\,(R_g + R_g\, kI_b + R_{gb}}\right)$$

$$= V\left(\frac{\dfrac{kR_{gb}}{(R_g + R_{gb})^2}}{\dfrac{[kR_g]}{(R_g + R_{gb})} + \dfrac{1}{I_b}}\right)$$

which is of the same form as eqn (2), with all terms apart from $V$ and $I_b$ constants.

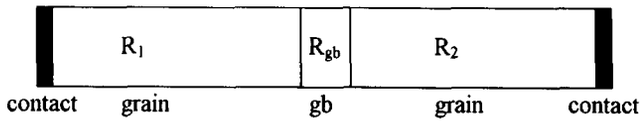


$R_g = R_1 + R_2$

**Fig. A1** Geometry used to obtain eqn (2), with $R_g = R_1 + R_2$.